Article

Pump-Shaped Dump Optimal Control Reveals the Nuclear Reaction Pathway of Isomerization of a Photoexcited Cyanine Dye

Benjamin Dietzek, Ben Brggemann, Torbjrn Pascher, and Arkady Yartsev

J. Am. Chem. Soc., **2007**, 129 (43), 13014-13021• DOI: 10.1021/ja072639+ • Publication Date (Web): 09 October 2007

J|A|C|S
ARTICLES
Published on Web 10/09/2007

Pump-Shaped Dump Optimal Control Reveals the Nuclear Reaction Pathway of Isomerization of a Photoexcited Cyanine Dye

Benjamin Dietzek,*,† Ben Brüggemann,‡ Torbjörn Pascher, and Arkady Yartsev

Contribution from the Department of Chemical Physics, Lund University, P.O. Box 124, SE-22100 Lund, Sweden

Received April 16, 2007; E-mail: dietzek@mit.edu

Abstract: Using optimal control as a spectroscopic tool we decipher the details of the molecular dynamics of the essential multidimensional excited-state photoisomerization — a fundamental chemical reaction of key importance in biology. Two distinct nuclear motions are identified in addition to the overall bond-twisting motion: Initially, the reaction is dominated by motion perpendicular to the torsion coordinate. At later times, a second optically active vibration drives the system along the reaction path to the bottom of the excited-state potential. The time scales of the wavepacket motion on a different part of the excited-state potential are detailed by pump-shaped dump optimal control. This technique offers new means to control a chemical reaction far from the Franck−Condon point of absorption and to map details of excited-state reaction pathways revealing unique insights into the underlying reaction mechanism.

Introduction

Isomerization, one of the simplest yet most general chemical reactions, is a key process in chemistry and biology.[1] Photoinduced *cis*−*trans* isomerization constitutes the first step in vision,[2] triggers photosynthesis in simple bacteria,[3] and is essential for light reception of green plants.[4] Isomerizing molecules are central for the quest of designing molecular electronics, e.g., optical memory and photooptical switches.[5,6] The omnipresence of isomerization reactions demands a detailed understanding of the intramolecular reaction pathway[7] and of the chromophore−protein interactions in biological systems[8] and initiated advanced theoretical studies of the potential energy surfaces of biological chromophores[9−11] and paradigm model systems.[12,13]

Very recently, optimal control has been applied to influence isomerization in the liquid phase[14,15] and in protein matrices.[8] Optimal adaptive feedback as suggested by Judson and Rabitz[16] proved to provide great capability in controlling chemical reactions with the design of pump-laser fields optimally suited to "solve" an experimentally imposed task. In a conventional optimal control experiment, a self-learning adaptive feedback loop is applied to iteratively generate the pump electric field that solves the system's Schroedinger equation in real time without a priori knowledge about the molecular Hamiltonian.[16−23] The optimized pump encodes information about the system parameters, which are of central importance for the reaction dynamics though they might be hidden behind more dominant features in conventional time-resolved experiments. Over the past decade, successful adaptive feedback control of various physical processes and chemical reactions has been demonstrated.[19−21,24−28] In many cases this has led to a more

† Present address: Department of Chemistry, Massachusetts Institute of Technology, 77 Massachusetts Avenue, Cambridge, MA 02139, USA.
‡ Present address: Department of Physics, Humboldt University at Berlin, Newtonstr. 15, DE-12489 Berlin, Germany.

(1) Sundstrom, V. *Prog. Quantum Electron.* **2000**, *24*, 187−238.
(2) Schoenlein, R. W.; Peteanu, L. A.; Mathies, R. A.; Shank, C. V. *Science* **1991**, *254*, 412−415.
(3) Gai, F.; Hasson, K. C.; McDonald, J. C.; Anfinrud, P. A. *Science* **1998**, *279*, 1886−1891.
(4) Rockwell, N. C.; Su, Y. S.; Lagarias, J. C. *Annu. Rev. Plant Biol.* **2006**, *57*, 837−858.
(5) Tamai, N.; Miyasaka, H. *Chem. Rev.* **2000**, *100*, 1875−1890.
(6) Ikeda, T.; Tsutsumi, O. *Science* **1995**, *268*, 1873−1875.
(7) Kukura, P.; McCamant, D. W.; Yoon, S.; Wandschneider, D. B.; Mathies, R. A. *Science* **2005**, *310*, 1006−1009.
(8) Prokhorenko, V. I.; Nagy, A. M.; Waschuk, S. A.; Brown, L. S.; Birge, R. R.; Miller, R. J. D. *Science* **2006**, *313*, 1257−1261.
(9) Gonzalez-Luque, R.; Garavelli, M.; Bernardi, F.; Merchan, M.; Robb, M. A.; Olivucci, M. *Proc. Natl. Acad. Sci. U.S.A.* **2000**, *97*, 9379−9384.
(10) Cembran, A.; Bernardi, F.; Olivucci, M.; Garavelli, M. *Proc. Natl. Acad. Sci. U.S.A.* **2005**, *102*, 6255−6260.
(11) Garavelli, M.; Celani, P.; Bernardi, F.; Robb, M. A.; Olivucci, M. *J. Am. Chem. Soc.* **1997**, *119*, 6891−6901.
(12) Sanchez-Galvez, A.; Hunt, P.; Robb, M. A.; Olivucci, M.; Vreven, T.; Schlegel, H. B. *J. Am. Chem. Soc.* **2000**, *122*, 2911−2924.
(13) Improta, R.; Santoro, F. *J. Chem. Theory Comput.* **2005**, *1*, 215−229.
(14) Vogt, G.; Krampert, G.; Niklaus, P.; Nuernberger, P.; Gerber, G. *Phys. Rev. Lett.* **2005**, *94*.
(15) Dietzek, B.; Bruggemann, B.; Pascher, T.; Yartsev, A. *Phys. Rev. Lett.* **2006**, *97*, 258301.
(16) Judson, R. S.; Rabitz, H. *Phys. Rev. Lett.* **1992**, *68*, 1500−1503.
(17) Bardeen, C. J.; Yakovlev, V. V.; Wilson, K. R.; Carpenter, S. D.; Weber, P. M.; Warren, W. S. *Chem. Phys. Lett.* **1997**, *280*, 151−158.
(18) Assion, A.; Baumert, T.; Bergt, M.; Brixner, T.; Kiefer, B.; Seyfried, V.; Strehle, M.; Gerber, G. *Science* **1998**, *282*, 919−922.
(19) Brixner, T.; Damrauer, N. H.; Niklaus, P.; Gerber, G. *Nature* **2001**, *414*, 57−60.
(20) Brixner, T.; Gerber, G. *ChemPhysChem* **2003**, *4*, 418−438.
(21) Herek, J. L.; Wohlleben, W.; Cogdell, R. J.; Zeidler, D.; Motzkus, M. *Nature* **2002**, *417*, 533−535.
(22) Geppert, D.; Seyfarth, L.; de Vivie-Riedle, R. *Appl. Phys. B* **2004**, *79*, 987−992.
(23) Manz, J.; Sundermann, K.; de Vivie-Riedle, R. *Chem. Phys. Lett.* **1998**, *290*, 415−422.
(24) Daniel, C.; Full, J.; Gonzalez, L.; Lupulescu, C.; Manz, J.; Merli, A.; Vajda, S.; Woste, L. *Science* **2003**, *299*, 536−539.
(25) Weinacht, T. C.; Ahn, J.; Bucksbaum, P. H. *Nature* **1999**, *397*, 233−235.
(26) Bruggemann, B.; Organero, J. A.; Pascher, T.; Pullerits, T.; Yartsev, A. *Phys. Rev. Lett.* **2006**, *97*, 208301.

10.1021/ja072639+ CCC: $37.00

detailed understanding of underlying molecular dynamics, though extracting the control mechanism from the optimized electric field is certainly a nontrivial task.[24] This is because conventional optimal control can influence the system only at the incident of light absorption or, in the case of a pump−dump process[29−32] experimentally realized as intrapulse pump−dump,[17,33,34] in close proximity to the Franck−Condon point, and answers to important questions about the molecular motion under the influence of the optimized pump field can be inferred only indirectly.

Optimal shaped-pump control of the *trans*−*cis* photoisomerization of the model system 1,1′-diethyl-2,2′-cyanine iodine (1122C) has been recently demonstrated.[15] It was shown that in agreement with theory[35] the reaction outcome, i.e., the number of photoisomers, is influenced by the momentum composition of the initially excited wavepacket.[15] However, due to the intrinsically limited interaction range of the shaped-pump pulse with the reactive system, important questions on the nuclear reaction dynamics remained unsolved from the previous study:[15] What are the details of the wavepacket's encounter with the conical intersection? How do ground- and excited-state vibrations influence the reaction? Does the excited-state dynamics involve optically active modes? To resolve these questions, we follow a novel experimental outline suggested by Gerber and co-workers, who recently presented a first attempt to influence a reaction within a pump-shaped dump−probe scheme[36] (Figure 1). This approach combines the advantages of conventional pump−dump−probe spectroscopy in intercepting a reaction along its path[37−39] and optimal control in employing tailored electric fields to enhance a particular reaction outcome as compared to the use of transform limited pulses.[16,18−20,22−24,40−42] Thereby, optimal control of the photoinduced isomerization closer to the decisive points of the reaction, i.e., further down along the reaction coordinate, is achieved. While conventional shaped-pump optimal control yields an integrated picture of the molecular response, the approach pursued here enables us to disentangle and visualize the different time scales and the momentum composition of wavepacket motion and assign the dynamics to distinct parts of the excited-state potential. Furthermore, the influence of ground- and excited-state vibrations to the observed dynamics can be detailed. Hence, a local view on the excited-state dynamics along the reaction coordinate during photoinduced isomerization arises contrasting the conventional picture obtained in a shaped-pump experiment. We show that the optimized pulse can be conceptually separated into a preparation part interacting with ground-state molecules prior to photoexcitation and a delayed expression part reflecting the dynamics of the excited-state wavepacket at large displacements along the reaction coordinate.

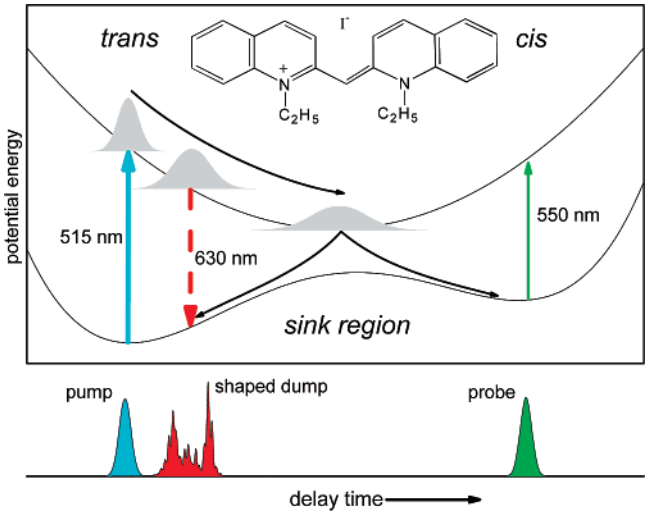

Figure 1. Experimental outline and the system under investigation, 1,1′-diethyl-2,2′-cyanine iodine, are presented schematically. Upon photoexcitation of the *trans*-isomer with a transform-limited pump pulse, the system evolves on the excited-state potential energy surface. At later times the Stokes shifted and optimized dump pulse most efficiently transfer the population back to the *trans*-ground state. Thereby the reaction channel is efficiently intercepted and the number of photoisomers produced reduced.

Experimental Section

The laser system and the basic experimental setup used for the optimal control experiments have been described elsewhere.[15,26] Briefly, the pulses of an amplified fiber oscillator (Clark, *CPA* 2001) are used to pump tunable noncollinear optical parametric amplifiers (TOPASwhite, Light Conversion, and NOPA, Clark) at a repetition rate of 1 kHz to generate the pump, dump, and probe pulses used in the experiment. The pump pulse was centered at 515 nm, the dump pulse was centered at 630 nm, and the probe was tuned to the *cis*-isomer absorption at 550 nm. At this wavelength, the appearance of the *cis*-isomer is probed at long delay times, while, at very short delays, contributions from ground state bleaching and stimulated emission are observed.[43] A 30-μm BBO crystal at the sample position was used to measure intensity autocorrelations and cross-correlations. Pulse shaping of the dump pulses was obtained by utilizing a 4f-zero dispersion compressor combined with a liquid-crystal array phase-only pulse-shaper (Jenoptik) placed in the Fourier plane of the compressor.[44] A self-learning adaptive feedback loop was employed to optimize the excitation pulses. Characterization of the resultant pulse shapes was done using sum-frequency generation cross-correlated frequency-resolved optical gating (xFROG) in the identical 30-μm BBO crystal at the sample position. As xFROGs were recorded with the optimized pump- and transform-limited probe pulses, the spectral-temporal features of the xFROG traces directly reflect changes in the pump pulse.[45]

1122C was used as provided by *SigmaAldrich* and dissolved in propanol of spectroscopic grade to yield an optical density of typically

(27) Meshulach, D.; Silberberg, Y. *Nature* **1998**, *396*, 239−242.
(28) Dudovich, N.; Oron, D.; Silberberg, Y. *Nature* **2002**, *418*, 512−514.
(29) Tannor, D. J.; Rice, S. A. *J. Chem. Phys.* **1985**, *83*, 5013−5018.
(30) Tannor, D. J.; Kosloff, R.; Rice, S. A. *J. Chem. Phys.* **1986**, *85*, 5805−5820.
(31) Tannor, D. J.; Rice, S. A. *Adv. Chem. Phys.* **1988**, *70*, 441−523.
(32) Vogt, G.; Nuernberger, P.; Selle, R.; Dimler, F.; Brixner, T.; Gerber, G. *Phys. Rev. A* **2006**, *74*, 033413.
(33) Cerullo, G.; Bardeen, C. J.; Wang, Q.; Shank, C. V. *Chem. Phys. Lett.* **1996**, *262*, 362−368.
(34) Dietzek, B.; Pascher, T.; Yartsev, A. *J. Phys. Chem. B* **2007**, *111*, 6034−6041.
(35) Hunt, P. A.; Robb, M. A. *J. Am. Chem. Soc.* **2005**, *127*, 5720−5726.
(36) Vogt, G.; Nuernberger, P.; Brixner, T.; Gerber, G. *Chem. Phys. Lett.* **2006**, *433*, 211−215.
(37) Gai, F.; McDonald, J. C.; Anfinrud, P. A. *J. Am. Chem. Soc.* **1997**, *119*, 6201−6202.
(38) Buckup, T.; Savolainen, J.; Wohlleben, W.; Herek, J. L.; Hashimoto, H.; Correia, R. R. B.; Motzkus, M. *J. Chem. Phys.* **2006**, *125*.
(39) Larsen, D. S.; van Stokkum, I. H. M.; Vengris, M.; van der Horst, M. A.; de Weerd, F. L.; Hellingwerf, K. J.; van Grondelle, R. *Biophys. J.* **2004**, *87*, 1858−1872.
(40) Rabitz, H.; de Vivie-Riedle, R.; Motzkus, M.; Kompa, K. *Science* **2000**, *288*, 824−828.
(41) Brumer, P.; Shapiro, M. *Annu. Rev. Phys. Chem.* **1992**, *43*, 257−282.
(42) Gruner, D.; Brumer, P.; Shapiro, M. *J. Phys. Chem.* **1992**, *96*, 281−290.
(43) Dietzek, B.; Yartsev, A.; Tarnovsky, A. N. *J. Phys. Chem. B* **2007**, *111*, 4520−4526.
(44) Weiner, A. M. *Rev. Sci. Instrum.* **2000**, *71*, 1929−1960.
(45) Trebino, R.; DeLong, K. W.; Fittinghoff, D. N.; Sweetser, J. N.; Krumbugel, M. A.; Richman, B. A.; Kane, D. J. *Rev. Sci. Instrum.* **1997**, *68*, 3277−3295.

0.5 at 525 nm in a 1-mm quartz cuvette. By recording absorption spectra, the integrity of the sample was ensured.

Results and Discussions

Dissolved in propanol, 1122C exhibits a 2.5-ps torsion motion from the Franck−Condon point to the bottom of the excited-state potential and an overall excited-state lifetime of about 16 ps. The photoreaction was initiated by a 50-fs transform limited pump pulse centered at 515 nm and thus slightly blue-shifted with respect to the absorption maximum at 524 nm. Upon photoexcitation excited-state bond twisting occurs, which moves the molecules along the reaction coordinate into a 90°-twist geometry. The differential absorption changes (ΔA) at 550 nm were probed at a 30-ps delay to monitor the formation of *cis*-isomers. For short delay times the same probe is dominated by ground-state bleach and stimulated emission.[43,46] The excited-state motion is accompanied by a strong Stokes shift of the stimulated emission.[43] In the control experiment, the isomerization quantum yield is changed by the 630-nm dump pulse, which is delayed in time with respect to the pump and resonantly interacts with excited molecules at large displacements along the bond-twisting reaction coordinate. It can intercept the reaction channel by dumping the excited-state population back to the ground state, and thereby it reduces the number of photoisomers produced.

Pump−Dump Probe Kinetics. Prior to adaptive pulse shaping, the reduction of the isomer formation by a delayed transform limited reference dump pulse has been studied (Figures 2A, S1). The pump−dump kinetics in Figure 2A corresponds to pump and dump pulse overlapping in time. To illustrate the delay-dependence of the dumping, Figure 2B displays the change of the photoisomerization yield as a function of the delay between the pump and reference-dump pulse in absolute and relative values. The dumping efficiency increases as a function of delay time and reaches a maximum of ∼22% at about 300 fs after photoexcitation.[47]

Ultrafast excited-state bond-twisting motion causing increasingly Stokes shifted stimulated emission is responsible for the initial rapid increase and successive decrease of the dumping efficiency. The reaction moves the excited population toward the bottom of the S_1-potential and thereby transiently populates the dumping window defined by the spectral position and width of the dump pulse.[43,48] At larger pump−dump separations a slow decay of the dump-efficiency curve is apparent, but even after 5 ps some dumping is preserved. It indicates that the relaxed excited-state population close to the bottom of the S_1 potential contains a high-energy emission tail extending to at least 630 nm. Therefore, the relaxed excited-state population is spread over a wider range of torsion angles than expected from previous studies.[43,48]

Pump-Shape Dump−Probe Optimal Control. Efficient control of the photoreaction far away from the Franck−Condon point is obtained by applying the recently demonstrated concept of a pump-shaped dump scheme.[36] Shaping the spectral phase of the dump pulse was done by means of a liquid-crystal array placed in the Fourier plane of a 4f-zero dispersion compressor.[44]

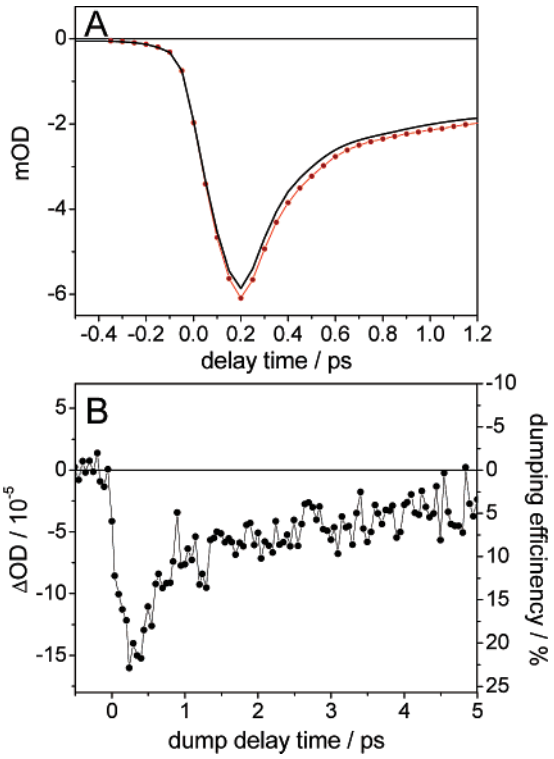

Figure 2. (A) Short time transient absorption kinetics recorded with (solid line) and without (line and symbols) the reference dump pulse. Pump and dump pulses were overlapping in time. (B) Dump induced changes in the ΔA signal at 30 ps as a function of pump−dump separation recorded with the reference-dump pulse. For comparison the right-hand axis shows the dumping efficiency as a function of pump−dump delay.

The optimization starts with the center of the (reference-) dump pulse delayed by 0.5 ps with respect to the pump pulse. However, it should be noted that this choice of starting condition does not affect the general applicability of the scheme employed, as the pulse shaper is capable of shifting any pulse in time without affecting its temporal shape by simply imposing a linear spectral phase.[36] The fitness used in the adaptive-feedback control experiment was defined as the number of photons in the pump pulse divided by the photoisomerization yield expressed as the ΔA signal at 550 nm and a 30-ps delay.[49]

Significant reduction of the photoisomer production can be achieved as shown in the inset of Figure 3, which displays the evolution of the fitness parameter during the control experiment. Notably, the random spectral phase imposed in the first generation of the genetic algorithm predominantly broadens the dump pulse and therefore stretches it to be in better spectral-temporal overlap with stimulated emission of the excited-state wavepacket as reflected in the experimentally determined dump efficiency (Figure 2). Hence, an on average higher fitness will be observed compared to the short reference pulse located at a delay of 500 fs. This explains that even in the first generation the average fitness is higher than the fitness obtained for the reference-dump pulse.

Using the optimized pulse train about 18% more efficient dumping as compared to the use of the reference pulse was achieved. This dumping is 1.4 times more efficient than that

(46) Rentsch, S. K. *Chem. Phys.* **1982**, *69*, 81−87.
(47) The differential absorption signal reflecting photoisomerformation at a 30 ps delay without dump pulse was measured to be 7×10^{-4}, while the maximum dump-induced change is 16×10^{-5}. Thus, 0.16/0.70 = 22%.
(48) Yartsev, A.; Alvarez, J. L.; Aberg, U.; Sundstrom, V. *Chem. Phys. Lett.* **1995**, *243*, 281−289.
(49) See Supporting Information

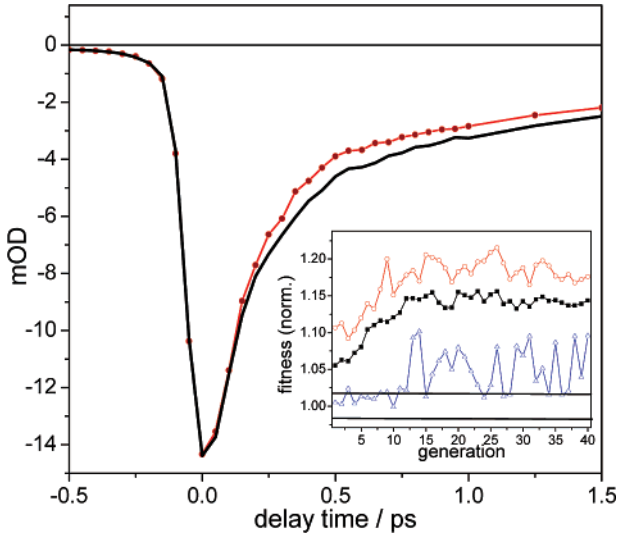

Figure 3. Short time scale of ΔA kinetics recorded at 550 nm with optimized (line and symbols) and reference dump pulse (line). Inset: Evolution of fitness parameter. Squares: average fitness. Circles: best fitness. Triangles: worst fitness per generation. The fitness was chosen as the integrated number of photons per pump pulse divided by the ΔA signal at 30 ps. The range of fitness obtained with the reference pulse is indicated by horizontal lines.

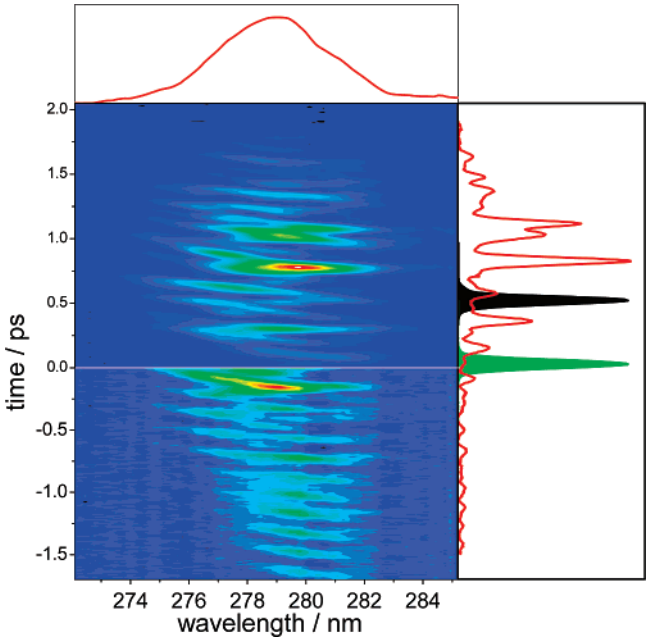

Figure 4. xFROG data of optimized dump pulse. For negative times the data are shown five times enlarged. Color coding: Blue refers to low and red to high sum-frequency intensities. On the right-hand side the intensity cross-correlation of the optimized dump pulse (red) is shown. In addition, the cross-correlation of the reference pulse (black) and the autocorrelation of the pump pulse (green) are displayed. Top panel: The time-integrated sum-frequency spectrum is shown.

achieved using the best-timed reference-dump pulse.[50] Hence, the effect of the optimized dump pulse exceeds the dumping efficiency of an optimally timed, transform limited reference pulse. This contrasts the results obtained in the first study on pump-shaped dump−probe spectroscopy,[36] where linearly chirped as well as freely shaped pulses result in the same dumping as the appropriately delayed transform limited dump pulse, and proves the capabilities of this promising emerging technique.

The complex pulse train ultimately obtained by adaptive feedback control is characterized by means of intensity cross-correlation and sum-frequency generation cross-correlated frequency-resolved optical gating (xFROG) at the sample position.[45] The xFROG sum-frequency signals, the cross-correlation traces of the optimized and reference dump pulse, and the autocorrelation of the 515-nm pump are shown in Figure 4. As the sum-frequency xFROG signals were recorded with the transform limited probe pulse, their dynamics directly reflect the spectral-temporal pulse shapes of the optimized dump pulses.[45]

Interestingly, the temporal profile of the optimized pulse is stretched so that *parts of the dump pulse interact with the sample prior to the pump pulse*.[51] As 1122C in its electronic ground state does not absorb photons at 630 nm, which is 60 nm red-shifted from the ground-state absorption cutoff at 570 nm, the prepump parts of the optimized pulse represent electronically nonresonant interactions with ground-state molecules. However, a distinct effect of the prepump pulses on the ΔA kinetics can be seen in Figure 3 (see also Supporting Information: Figure S2), where the kinetics recorded with the optimized pulse are compared to kinetics recorded with a reference pump delayed by 0.5 ps with respect to the pump. Up to about 200 fs after photoexcitation both traces are identical (Figure 3A). This directly shows that the initial overall excited-state population is not altered by the first part of the dump pulse. At 200 fs the kinetics start to deviate and the ΔA amplitude is significantly reduced though the dominant part of the dump pulse centered at ∼700 fs has not interacted with the sample yet. Thus, the deviation between the two transients reflects the reduction of the excited-state population induced by the prepump part of the shaped dump pulse. As the overall number of molecules promoted to the excited state is unaffected by the prepump part of the dump pulse, the significant changes in the isomerization kinetics cannot be understood simply as a reduced excitation efficiency.[52] Instead, a coherent control mechanism invoking the internal molecular degrees of freedom will be considered in the following.

In order to understand the molecular mechanism leading to efficient control of the isomerization reaction far away from the Franck−Condon point, we analyze the frequency content of the optimized pulse train. To do so, the xFROG data of the dump pulse (Figure 4A) as a function of time was split into two parts: The part preceding the pump interaction and the part of the dump pulse that interacts with the sample after the 515-nm excitation pulse. Remarkably, the time structures of the two subpulse trains reveal different characteristic frequencies. While the prepump part of the dump pulse exhibits a prominent mode

(50) Using the optimized pulse train, about 18% more efficient dumping as compared to the use of the reference dump was achieved. This corresponds to 15% = 18% × (1 − 0.15) more efficient dumping when referenced to the ΔA signal without any dump. So the efficiency of the optimized pulse compared to the reference pulse is equal to the total dumping, i.e., dumping of reference pulse (15%) and dumping compared to reference pulse (0.15%), divided by the dumping of the reference pulse, i.e., 15%. Thus the optimized pulse is twice as efficient in dumping compared to the 500-fs delayed reference pulse. Compared to the dumping efficiency of an optimally timed, transform limited reference pulse, optimal control results in dump-pulse shapes whose dump efficiency is still (0.15 + 0.15)/0.22 ≈ 1.4 times larger.

(51) Care was taken to ensure the reproducibility of the critical features of the optimized pulses as discussed in this manuscript. The appearance of the pre- and postpulse structures with the characteristic spectral contents was observed in three independent experimental runs.

(52) Prokhorenko, V. I.; Nagy, A. M.; Miller, R. J. D. *J. Chem. Phys.* **2005**, *122*.

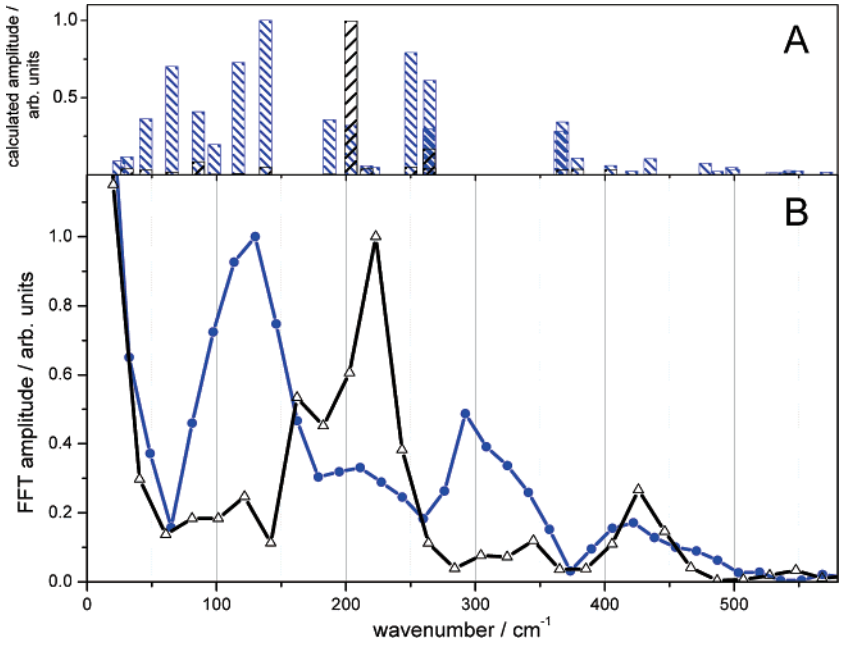

Figure 5. (A) Results of DFT calculations. The vibrational frequencies obtained are indicated by bars. Their respective amplitudes are scaled according to the dump-pulse spectrum. The spectrum of modes involving a tilting deformation (in-plane stretch) of the cyanine bridge is shown in blue (black).[49] (B) Frequency content of optimized dump-pulse train. Amplitudes obtained from Fourier transformation of parts of the pump-pulse interacting before (triangles) and after (circles) the 515-nm pump pulse.

contribution at 220 cm^{-1}, the temporal envelope of the trailing side of the dump pulse is dominated by two modes at 130 and 300 cm^{-1}.

Interestingly, a previous experiment demonstrating optimal control of *trans*−*cis* isomerization in 1122C in solution using a conventional shaped-pump approach yielded identical frequency compositions of the optimized pulses.[15] In this experiment we found that the pulse train best suited for diminishing the isomerization yield was dominated by a 200 cm^{-1} mode, corresponding to the 220 cm^{-1} mode present in the prepump part of the optimized dump pulse (Figure 5). On the contrary, increased isomer formation was observed, when the pump pulse contained modes at 130 and 320 cm^{-1}.[15] The authors of ref 35 predicted that the isomerization yield in cyanines can be reduced when the system is forced to move along a coordinate orthogonal to the dominant reaction coordinate thereby encountering an extended conical intersection seam on the *trans* side of the ground-state potential. However, when modes are populated that prevent the system from reaching the conical intersection (CI) before having relaxed toward the "*cis* side" of the excited-state potential, an increase of the isomerization yield is observed.[35] Along these lines, the experiment in ref 15 was interpreted as altering the initial momentum composition of the photoexcited wavepacket and consequently influencing the dynamics on the multidimensional excited-state potential.[12,13,35] It should be noted that the C−N stretch mode considered in the theoretical work on a cyanine model system by Hunt and Robb is characterized by a wavenumber of 1900 cm^{-1}. Thus the frequency is far outside the spectral bandwidth of the dump pulses used in our experiment or the pump pulses in ref 15. However, as will be discussed in detail below, these differences in wavenumbers are attributed to the different molecular species under consideration and do not alter the agreement between experiment and theory.

The striking similarities of the pulse characteristics in this work to the pulse train structures in ref 15 will be the starting point for the discussion of the pump-shaped dump experiment presented here. The distinctly different frequency contents of the pre- and postpump parts of the optimized dump pulse show that two conceptually different molecular mechanisms are addressed in the control experiment independently and successively, as discussed in the following.

First, we will consider the influence of the prepump parts of the dump pulse. As the 630-nm dump pulse is in resonance with neither ground state *trans*- nor *cis*-1122C, the leading part of the pulse can interact only nonresonantly with the 1122C ground-state population. We suggest that it excites a vibrational wavepacket on the S_0-potential by successive stimulated Raman scattering events.[53,54] Successive stimulated Raman scattering interactions are timed to the evolution of the 220 cm^{-1} mode wave packet. Therefore, constructive interference enhances nuclear motion along this coordinate. Coherence in other modes, i.e., the modes 130 at 300 cm^{-1}, which are also covered by the spectral width of the dump pulse, is not preserved due to destructive interference as the interaction with individual parts of the dump pulse are out off phase with respect to these vibrations (Figure 5). Thus, as a net effect the prepump part of the dump pulse prepares a ground-state wavepacket with momentum stored in the 220 cm^{-1} mode, while the other modes remain unaffected. As the resonant 515-nm pump pulse is shorter than the vibrational period with a characteristic wavenumber of 220 cm^{-1}, the excitation transfers the momentum of the ground-state wavepacket to the first excited state, while leaving the overall population transfer efficiency unaffected (Figure 3). Consequently, upon photoexcitation the system

(53) Dhar, L.; Rogers, J. A.; Nelson, K. A. *Chem. Rev.* **1994**, *94*, 157−193.
(54) Dietzek, B.; Grafe, S.; Schmitt, M.; Yartsev, A.; Pascher, T.; Sundstrom, V.; Kiefer, W.; Ivanov, M. Y. *Phys. Rev. Lett.* **2007**, *98*, 187402.

starts to evolve along the coordinate of the 220 cm^{-1} mode on the S_1 potential. Thereby, the system reaches the CI seam in proximity to the FC region. As the encounter with the CI seam occurs at torsion angles close to the *trans* geometry, the population undergoes internal conversion directly back to the thermodynamically stable *trans* ground state. Thus, the preparation part of the optimized dump induces a ground-state wavepacket, whose effect on the isomerization reaction results in a reduced quantum yield of isomerization.[12,13,35]

To gain insight into the nature of the vibrational modes active in the optimal control experiment, a density functional theory calculation using GAUSSIAN 03[55] for the positively charged *trans*-1122C, neglecting the iodine anion was carried out using the B3LYP functional and the basis set 6-31(d,p). The low-wavenumber vibrations obtained from the optimized ground-state geometry can be grouped into three subsets based on the changes they induce on the central methine bridge of 1122C. Modes that do not exhibit any action on the central part of the molecule will not be discussed further. The remaining vibrations are grouped into vibrations, which involve the tilting motion of one of the central C−C bonds and those that only involve in-plane stretching vibrations of the central part of the methine bridge without affecting the mutual orientation of the quinoline rings. The results of the DFT calculations are presented in Figure 5A, where the calculated modes falling within the laser bandwidth are shown. Their respective calculated amplitudes are scaled by multiplication with the normalized spectrum of the dump pulse.

As can be seen from Figure 5A, there are numerous twisting vibrations in the region 50−500 cm^{-1}, which are covered by the dump-laser spectrum. However, there is only one strong bond-stretching vibration located at 202 cm^{-1}, which is the symmetric stretch of the whole molecule and thus corresponds to the 1900 cm^{-1} C−N stretching vibration considered in ref 35.[56] It is consequently identified with the 220 cm^{-1} vibration visible in the prepump part of the optimized dump pulse. This mode represents the dominant cyanine-bridge stretching as a part of the symmetric stretching mode of the whole molecule within the laser bandwidth. Thus, it can be concluded that the prepump part of the dump pulse has been optimized to create a ground-state wavepacket in a vibrational mode perpendicular to the torsional bond-twisting motion. Furthermore, the nuclear displacements upon excitation of the 202 cm^{-1} mode closely resemble the characteristics of the C−N stretching mode calculated by Hunt and Robb for a model cyanine.[35] Therefore, our calculations are coherent with previous theoretical results. The result proves that the vibration promoting an early encounter of the excited-state wavepacket with the CI seam involves significant in-plane stretching of the central cyanine bridge, as theoretically derived in ref 35 and speculated in ref 15.

In contrast to previous work on conventional optimal control employing shaped pump pulses,[15] the pump-shaped dump−probe experiment presented here allows us to differentiate between the motions on different parts of the excited-state PES. Thereby, the time scale of motion along the promotion mode toward the CI seam, i.e., perpendicular to the torsion coordinate, can be quantified: The identical ΔA kinetics recorded for the reference and the optimized dump pulse for short delay times indicate that up to 200 fs the excited-state population is not affected by the excitation of the 220 cm^{-1} vibration but later the kinetics start to deviate (Figure 2B). Hence, it takes for the system 200 fs to evolve along the promoting mode and perpendicular to the torsion reaction coordinate before the population starts to encounter the CI seam. Furthermore, the absence of additional stepwise deviations of the transients recorded with the optimized and reference dump pulse (Figure 3) indicates only one encounter with the CI seam at geometries corresponding to a *trans* side of the ground-state potential is observed.

However, not the entire population is found to pass through the CI seam. Previously it was shown that excitation of modes at 130 and 300 cm^{-1} most efficiently keeps the system from encountering the CI before arrival at the bottom of the excited-state PES.[15] The approximately 400 cm^{-1} spectral width of the pump pulse itself is broad enough to directly excite a vibrational wavepacket on the S_1 potential including the 130 and 300 cm^{-1} modes as well as the 220 cm^{-1} mode.

In contrast to the 202 cm^{-1} mode, the nature of the 130 and the 300 cm^{-1} modes is characterized by mutual out-of-plane motion of the quinoline groups, typically associated with molecular motion of torsion character. Therefore, the 130 and 300 cm^{-1} modes detain the photoexcited wavepacket from an encounter with the CI seam at early times by predominantly steering the population toward the bottom of the excited-state PES. The momentum initially placed in the 130 and 300 cm^{-1} detaining modes by the short pump pulse is revealed by the dump pulse, which expresses the coherent oscillations in these modes. The efficient downhill motion of the excited-state population induced by the 130 and 300 cm^{-1} modes is directly reflected in the xFROG trace of the postpump expression part of the optimized dump pulse (Figure 4). A coherent wavepacket motion on the excited-state PES involving modes with bond-twisting character moves the population through the spectral window accessible for dumping from a larger energetic separation of the potential energy surfaces to smaller ones in one-half-period of the oscillation and *vice versa* during the second half-period. Therefore, a pulse train, in which two successive subpulses exhibit opposite chirp, is expected to most efficiently dump the excited-state population coherently oscillating along the FC-active bond-twisting reaction coordinate. This is apparent in the xFROG data (Figure 4) experimentally confirming that the observed oscillations are associated with modes moving the system efficiently along the bond-twisting reaction coordinate, along which the S_1-S_0 energetic separation varies notably. Therefore, the vibrational motion of the excited-state wavepacket remaining on the S_1 potential at large bond-twisting angles will be most efficiently dumped by locking the temporal structure of the dump pulse to the internal clock provided by the these intramolecular vibrations.

The unique capabilities of pump-shaped dump−probe spectroscopy of discriminating between different parts of the excited-state PES result in a detailed optimal control mechanism. The experimental outcome comprises the results of previous work and qualitatively illustrates the validity of recent theoretical studies predicting the multidimensionality of the excited-state

(55) Frisch, M. J., et al. *Gaussian 03*, revision C.02; Gaussian, Inc.: Wallingford, CT, 2004.

(56) It should be noted that mode shifts upon photoexcitation of the dye are not taken into account in the pure ground-state calculations performed here. However, the position of the 202 cm^{-1} mode, which is excited by stimulated Raman scattering in the ground-state potential, will not be affected by this fact.

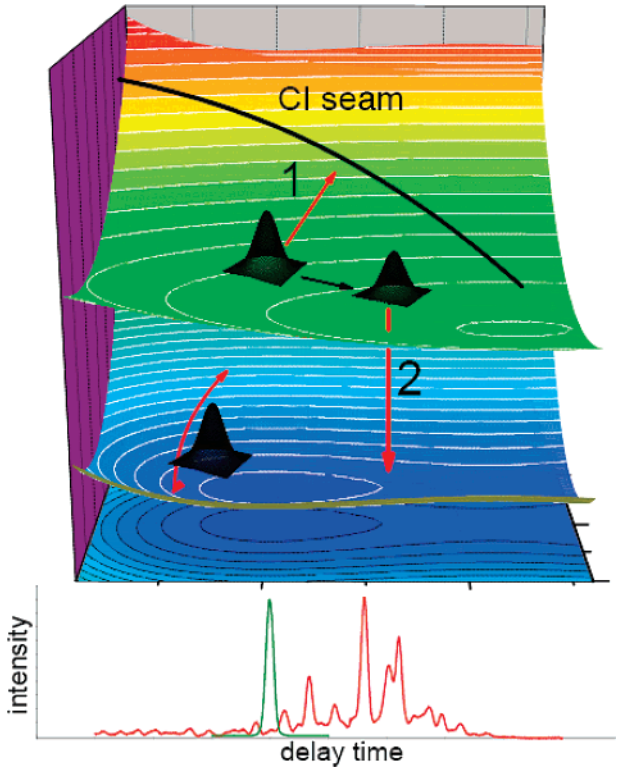

Figure 6. Schematic picture of the control mechanism achieved by the complex dump pulse is shown.

PES in cyanines to be of importance for a detailed understanding of the photoisomerization reaction.[12,13,35] However, the study at hand offers conceptually novel insight into the role of individual modes in the photoreaction by assigning the vibrational coherences to the ground- and excited-state PES. Figure 6 schematically depicts the joint molecular mechanism as suggested to account for the observed reduction of the number of excited molecules reaching the bottom of the S_1 potential and thereby the number of photoisomers produced. Importantly, two distinct light-matter interactions are incorporated into a single optimized dump pulse: (i) nonresonant preparation of a vibrational wavepacket in the promoting vibration by stimulated Raman scattering and (ii) resonant population transfer by stimulated emission. While the initial nonresonant part of the dump pulse interacts with the ground-state population, the trailing side of the shaped dump resonantly interacts with the excited-state population. As the excited-state wavepacket oscillates coherently in modes with typical torsion character, optimized dumping is achieved by locking the temporal structure of the dump-pulse envelope to the wavepacket dynamics in the detaining modes. It should be emphasized that the nonresonant interaction does not change the shape of the potential energy surfaces as observed in experiments employing the dynamical AC-Stark effect.[57] As a joint result of the two conceptually different control mechanisms and the interaction with particular vibrational modes with distinct character, the reactive channel is most efficiently blocked and the isomerization yield reduced.

In a subsequent experiment we imposed the task of maximizing the number of *cis*-isomers produced in the photoreaction to the adaptive feedback loop. The resultant dump pulse is rather short in time (cross-correlation width ~180 fs) and characterized by a dominant up-chirp (Figure S3). This finding can be rationalized considering the spectral-temproal evolution of the stimulated emission (fluorescence) in photoexcited 1122C and related systems.[43,48] After photoexcitation the excited-state population relaxes to the bottom of the S_1 potential, and this characteristic bond-twisting motion is accompanied by a significant Stokes shift of emission. Thus, the spectral evolution within the up-chirped dump pulse will oppose the evolution of the emission wavelength associated with the excited-state relaxation.[17,43,58] Thereby, the least efficient dumping is achieved. Despite the conceptually straightforward result and the well-understood structure of the anti-optimized pulse, the ΔA signal at 30 ps rose only marginally by 2%.

Conclusion

The nuclear reaction pathway of photoinduced excited-state isomerization dynamics in the model system 1,1′-diethyl-2,2′-cyanine iodine was deciphered by successful implementation of the pump-shaped dump-control scheme.[36] By applying this recently developed approach, a complexly shaped dump pulse addressing the intramolecular degrees of freedom is obtained to efficiently control isomerization in the liquid phase. The data allow us to disentangle the time scales and nature of wavepacket motion and assign them to different parts of the excited-state potential. In contrast to conventionally employed optimal control, which leads to an *integrated picture* of the molecular response to the shaped electric field of the pump pulse, the approach of pump-shaped dump−probe spectroscopy conceptually yields a *local view* on the reaction dynamics. In conclusion, a pump-shaped dump experiment offers two particular advantages over the conventional approach employing shaped pump pulses: First, it allows us to influence the reaction at larger values of the reaction coordinate and thus in closer proximity to the decisive moments of the reaction. Second, more detailed information on the reaction dynamics is revealed directly, by selectively using the shaped dump in the spectral region of stimulated emission, which is coupled to a defined S_n-S_0 (typically S_1-S_0) transition.

Using adaptive feedback control in the pump-shaped dump−probe scheme the photoisomerization yield of the paradigm system 1,1′-diethyl-2,2′-cyanine iodine could be efficiently reduced. The effect of the optimized dump pulse can be divided into two fundamentally different interactions: (i) prior to the pump-pulse interaction the nonresonant dump pulse excites the 202 cm^{-1} fundamental symmetric stretching mode of the whole molecule including the methine bridge on the ground-state potential by stimulated Raman scattering. The ground-state wavepacket is resonantely transferred to the excited state by the short transform limited pump pulse. There, the momentum along the detaining mode leads to an encounter of the excited-state wavepacket with an extended CI seam after 200 fs and a loss of the excited-state population within 300 fs after photoexcitation. (ii) Population evolving on the excited state after about 300 fs is most efficiently dumped by a dump pulse, which addresses low-frequency vibrational modes that bear torsion character. Thus, these modes at 130 and 300 cm^{-1} reflect the

(57) Papastathopoulos, E.; Strehle, M.; Gerber, G. *Chem. Phys. Lett.* **2005**, *408*, 65−70.

(58) Bardeen, C. J.; Yakovlev, V. V.; Squier, J. A.; Wilson, K. R. *J. Am. Chem. Soc.* **1998**, *120*, 13023−13027.

coherent wavepacket motion that keeps the system from encountering the CI before arrival at the bottom of the excited-state PES. Hence, a dual-purpose optimized pulse is observed incorporating both nonresonant interaction of the shaped dump pulse with the ground-state population and resonant interaction with the excited-state population into a single optimized pulse train. We believe that applying the pump-shaped dump scheme will allow control of a broad range of excited-state branching reactions by efficient blocking of one of the reactive channels at large values of the reaction coordinate. Thus this emerging experimental outline offers optimal control at large amplitudes of the reaction coordinate and thus in situations where the conventional shaped-pump control might not be applicable. The approach is easily extended to mapping the excited-state dynamics over a wide range of the reaction coordinate in systems, in which the reaction is accompanied by significant changes of the emission band. Though the full potential of this promising technique remains to be explored, this experimental route potentially yields a much more detailed picture of the underlying control mechanism and thus of the decisive moments and critical features of a chemical reaction compared to conventional shaped-pump control.

Acknowledgment. This work was financed by the Swedish Research Council, the Crafoord Foundation, and the Alice and Knut Wallenberg Foundation. Stimulating discussions with Villy Sundström and Tõnu Pullerits are highly acknowledged. B.D. gratefully acknowledges financial support of the Alexander-von-Humboldt Gesellschaft.

Supporting Information Available: Transient absorption kinetics plot with and without reference dump pulse, differential absorption kinetics plot with optimized and reference dump pulse at 500 fs, xFROG data of anti-optimized pulse, chemical structure of 1122C, and additional information regarding characterization of the optimized dump pulse, experimental details, choice of fitness, and categorization of molecular vibrations. Also, complete citation for ref 55. This material is available free of charge via the Internet at http://pubs.acs.org.

JA072639+